

# Spatio-temporal variation in leaf area index in the Yan Mountains over the past 40 years and its relationship to hydrothermal conditions

Da Guo<sup>a,b,c</sup>, Xiaoning Song<sup>a,b,\*</sup>, Ronghai Hu<sup>a,b</sup>, Rui Ma<sup>d</sup>, Yanan Zhang<sup>a,b</sup>, Liang Gao<sup>a,b</sup>, Xinming Zhu<sup>a,b</sup>, Paul Kardol<sup>c</sup>

<sup>a</sup> College of Resources and Environment, University of Chinese Academy of Sciences, Beijing 100049, China

<sup>b</sup> Beijing Yanshan Earth Critical Zone National Research Station, University of Chinese Academy of Sciences, Beijing 101408, China

<sup>c</sup> Department of Forest Ecology and Management, Swedish University of Agricultural Sciences, Umeå, Sweden

<sup>d</sup> School of Remote Sensing and Information Engineering, Wuhan University, Wuhan 430079, China

## ARTICLE INFO

### Keywords:

Mountains  
Climate change  
Leaf area index  
Vegetation greening  
Global warming  
Precipitation

## ABSTRACT

Changes in hydrothermal conditions have significant effects on vegetation, but there is still a lack of understanding of how vegetation responds to land surface (surface temperature and soil moisture) and meteorological (temperature and precipitation) conditions in mountain regions. This study examined the trends of leaf area index (LAI) in the Yan Mountains over the last four decades using Global Land Surface Satellite (GLASS) data. The results showed a persistent increase of LAI (greening) over 20 % to 80 % of the study area in growing season, spring, summer and autumn. Anthropogenic activities caused the greening trend by crop management before 2000 and afforestation after 2000. The increasing rate of LAI varied with elevation, and the most significant increase occurred in areas between 300 and 900 m, and the lowest increase occurred in areas below 300 m. Moreover, we found that LAI was negatively correlated with land surface temperature and soil moisture, but positively correlated with precipitation and air temperature. The time-lag effect was found between hydrothermal factors and LAI in the past four decades. There was a time lag of 2–3 months between LAI changes and temperature/precipitation during the early and late stages of the growing season, and a time lag of 0–1 month during the middle stage. Specifically, there was no time lag in vegetation response to surface soil moisture, and a time lag of 2–3 months in vegetation response to land surface temperature from July to October. Our findings provide insights into how vegetation adapts to land surface and climatic hydrothermal conditions in mountain regions and can be used by governments to develop policies for ecological protection.

## 1. Introduction

Vegetation is a vital link between terrestrial ecosystems and the atmosphere, connecting moisture, temperature, carbon and energy. It provides humans with essential resources, such as food, fuel and fiber (Pei et al., 2021; Piao et al., 2019). The variation in vegetation structure and function would affect the biodiversity and energy supply, and also provide important information about ecological feedback to climatic changes such as hydrothermal change and anthropogenic factors such as land-use change (Wang et al., 2020). Given the essential role of vegetation in regulating climate change by absorbing carbon dioxide from the atmosphere (Tucker et al., 1986), it is significant to quantify the temporal and spatial changes in vegetation and analyze its drivers.

Leaves are the primary plant organs responsible for photosynthesis.

The leaf area index (LAI) is a measure of the one-sided area of green leaves per unit of horizontal ground area (Chen and Black, 1992; Yan et al., 2019). The LAI is important as it can reveal the magnitude of leaves, the structural characteristics of vegetation, the growth status of vegetation, and carbon cycling (Chen et al., 2019b). Satellite observations are an effective measurement to monitor changes in terrestrial ecosystems because of their large area coverage and short revisit intervals (Piao et al., 2003; Piao et al., 2015). At present, the main long-term global LAI products include CYCLOPES LAI (Baret et al., 2007), MODIS LAI (Myneni et al., 2015), GIMMS3g (Zhu et al., 2013) and GLASS LAI (Xiao et al., 2014). Although some studies have used CYCLOPES LAI, GIMMS LAI and MODIS LAI in studying vegetation dynamics (Piao et al., 2015; Zhu et al., 2017), GLASS LAI has good quality pixels and smooth LAI profiles on rugged surfaces (Jin et al.,

\* Corresponding author at: College of Resources and Environment, University of Chinese Academy of Sciences, Beijing 100049, China.

E-mail address: [songxn@ucas.ac.cn](mailto:songxn@ucas.ac.cn) (X. Song).

<https://doi.org/10.1016/j.ecolind.2023.111291>

Received 16 September 2022; Received in revised form 25 October 2023; Accepted 16 November 2023

Available online 24 November 2023

1470-160X/© 2023 The Authors. Published by Elsevier Ltd. This is an open access article under the CC BY license (<http://creativecommons.org/licenses/by/4.0/>).

2017) and long time span (from 1981 to 2021), making it the preferred choice to study the greening trend of vegetation and its response to hydrothermal conditions in the Yan Mountains in the past 40 years.

Monitoring the dynamics of LAI and its responses to climatic changes and human activities are of great importance for implementing effective strategies for vegetation rehabilitation. On the one hand, climatic factors, especially temperature and precipitation patterns, drive changes in vegetation by altering land surface temperature and soil moisture conditions (A et al., 2016; Wang et al., 2020). That means land surface temperature and moisture have a more direct impact on vegetation than precipitation and air temperature (Wang et al., 2018). Several studies have shown that air temperature and precipitation had a significant impact on vegetation LAI (Afuye et al., 2022; Antala et al., 2022; Li et al., 2014; Li et al., 2021; Mao et al., 2012; Piao et al., 2006), but the influence of land surface temperature and surface soil moisture on vegetation LAI has not yet been systematically studied. Moreover, studies focused on the effects of simultaneous hydrothermal changes on vegetation, with little attention on the time-lag effects (Wu et al., 2015). Therefore, the impact of air temperature, precipitation, land surface temperature and surface soil moisture on vegetation LAI and its time-lag effect needs to be further studied.

On the other hand, human activities also play a role in vegetation changes (Jiang et al., 2020; Wang et al., 2021). Since 2001, the Chinese government has implemented a large number of vegetation restoration projects, such as the Three-Norths Shelter Forest Project, the Beijing-Tianjin Sand Source Restoration Project and the Grain to Green Project (Li, 2004; Wang et al., 2007). Although several studies have already identified these strategies significantly contributed to the greening trend as a whole in China (Chen et al., 2019a; Piao et al., 2019; Zhu et al., 2016), the greening trend caused by these strategies implementation showed a significant spatial heterogeneity because of the large topography difference of China, particularly in mountainous regions. The air temperature, precipitation, land surface temperature and soil moisture conditions can greatly vary over small spatial scales in mountainous regions (Wang et al., 2021) due to the large terrain undulations. Therefore, considering the LAI variations of mountainous regions could provide references to formulate and implement optimal ecological protection policies in mountainous regions.

In this context, the main aim of this study was to monitor the greening trend of vegetation in the Yan Mountains during the last four decades by GLASS LAI remote sensing data and quantify the response of vegetation LAI to variation/fluctuation in plant types, terrain, temperature and moisture. Specifically, we focused on four issues: (1) The spatial and temporal changes in LAI in the growing season, spring, summer, and autumn. (2) The impact of terrain on the vegetation greening trend and plant type fluctuation. (3) The response of LAI to air temperature, precipitation, land surface temperature and soil moisture. (4) The time lag between LAI and moisture and temperature at different seasons.

## 2. Materials and methods

### 2.1. Study area

The study area is a part of the Yan Mountains, which is situated between 115°02'E-122°13'E and 39°38'N-43°15'N (Fig. 1), covering five provinces, such as Inner Mongolia, Hebei, Beijing, Tianjin, Liaoning. The altitude ranges from -83 m to 2059 m. The Yan Mountains has a temperate continental monsoon climate. From 1981 to 2020, the average temperature and total precipitation during the growing season were 16–18 °C and 340–600 mm, respectively. Currently, forestland, cropland and grassland are the most dominant land cover types in the Yan Mountains, accounting for approximately 90 % of the total area. The Yan Mountains is located in semi-humid and semi-arid climatic zones, has a very fragile ecology, and its vegetation is extremely sensitive to hydrothermal changes, thus it can be utilized as an experimental area for monitoring the responses of mountain vegetation to hydrothermal changes.

### 2.2. Data sources

#### 2.2.1. Leaf area index

The GLASS LAI data (Xiao et al., 2014) used in this study were acquired from the National Earth System Science Data Center, China. In the past 40 years, there was no one LAI product that was produced from the constant satellite sensor and had the same spatial resolution spans from 1981 to 2020. In order to analyze the LAI dynamics around 2000, which is the year that vegetation restoration projects were implemented, we separated these 40 years into two stages: from 1981 to 2000 and from 2001 to 2020. We selected the GLASS LAI product derived from AVHRR for the period 1981–2000, which had a spatial resolution of 0.05° and a temporal resolution of 8 days. The GLASS LAI product derived from MODIS, with a spatial resolution of 500 m and 8-day interval, was chosen to analyze the vegetation LAI dynamics for the period 2001–2020. The finer spatial resolution of LAI data is beneficial for detecting the variations of vegetation in small areas because the moderate spatial resolution of LAI data may ignore the changes on a small scale and include a large spatial heterogeneity in mountain areas.

We also created a monthly LAI dataset, using the maximum LAI value in each month. During 2001–2020, the monthly LAIs were aggregated to grid cells of 1 × 1 km using the spliced 500 m resolution data. We calculated the growing season LAI (LAI<sub>GS</sub>) by averaging the monthly LAI from April to October. Spring LAI was calculated by averaging the monthly LAI from April to May, while summer LAI was calculated by averaging the monthly LAI from June to August. Finally, autumn LAI was determined by averaging the monthly LAI from September to October.

#### 2.2.2. Climate data

The hydrothermal data, including average air temperature and total

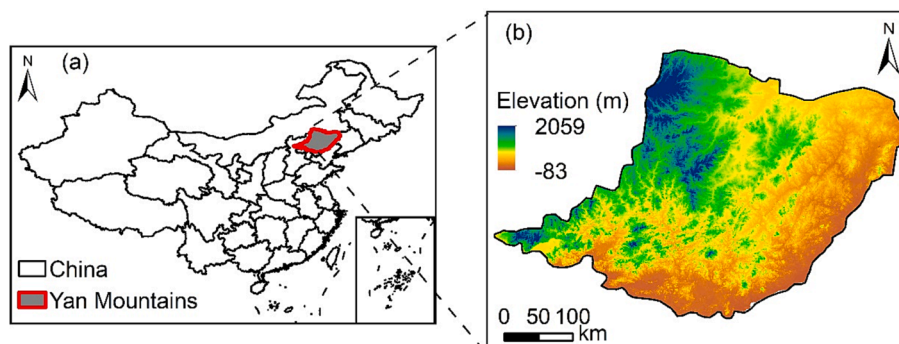


Fig. 1. Location of the study area (a) and a digital elevation model for the region (b).

precipitation (Peng et al., 2019), were acquired from the Loess Plateau SubCenter at the National Earth System Science Data Center, National Science & Technology Infrastructure of China (<https://loess.geodata.cn>). The data has a monthly temporal resolution, and the spatial resolution is 1 km. To match the spatial resolution of the hydrothermal data and the LAI data, we employed the nearest resampling method to resample the temperature and precipitation data to a resolution of 0.05° between 1981 and 2000 and 1 km between 2001 and 2020.

### 2.2.3. Land surface data

Land surface thermal and moisture data used in this study include land surface temperature (LST) and surface soil moisture (SSM). LST was derived from MOD11A2, with a spatial resolution of 1 km and an 8-day interval from 2001 to 2020. LST was obtained from the Google Earth Engine (GEE) Cloud Platform (<https://earthengine.google.com>), which contains a wealth of remote sensing datasets and has powerful data processing capabilities. We preprocessed the data through GEE, including data stitching, resampling, and cropping. SSM was derived from the ERA5 monthly averaged data on single levels (<https://cds.climate.copernicus.eu>), which provides four layers of soil moisture. We obtained the volume of water ( $\text{m}^3/\text{m}^3$ ) in the topsoil layer (0–7 cm) from 2001 to 2020 because the main limitation of remote sensing techniques is that only the surface soil moisture (the top 5 cm of the soil column) can be estimated (Peng et al., 2017). The ERA5 soil moisture datasets have a monthly temporal resolution and spatial resolution of 0.1°. To match the spatial resolution of LAI, we resampled the soil moisture data to a spatial resolution of 1 km using the bilinear interpolation method.

### 2.2.4. Digital elevation model

Digital elevation model (DEM) data were downloaded from the Resource and Environment Science and Data Center (<https://www.resdc.cn>), with a spatial resolution of 1 km. We used the DEM data to study the effects of altitude on the LAI trend.

### 2.2.5. Land cover data

A land cover map of the Yan Mountains was extracted from the Global 30-m land-cover dynamic monitoring products with fine classification system from 1985 to 2020 (GLC\_FCS30-1985–2020) (Zhang et al. (2021); Zhang et al., 2021b), which was downloaded from CASEarth (<https://data.casearth.cn>). The map has a spatial resolution of 30 m and a temporal resolution of 5-year. The vegetation types in the study area include cropland, broadleaved forest, needle-leaved forest, herbaceous cover, grassland, sparse vegetation and wetlands. The land cover data were resampled using the nearest neighbor method to match the spatial resolution of LAI.

## 2.3. Data analysis

The temporal changes in LAI during the growing season and across the three seasons (i.e., spring, summer, and autumn) were calculated using the least squares linear regression method. The slope of the regression indicates the rate of change in LAI over time (Li et al., 2020). If the slope value is greater than zero, it indicates an increasing trend (greening); if the slope value is less than zero, it indicates a decreasing trend (browning) (Zhu et al., 2016). To quantify the spatiotemporal patterns of LAI, we applied Sen's slope trend analysis for the period 1981–2020 (Gang et al., 2014; Ma and Frank, 2007). The significance level ( $z$  value) of LAI trends was calculated by Mann-Kendall (M–K) test, and the significance level of  $\alpha = 0.05$  ( $|z| \geq 1.96$ ) was selected to recognize the significance of LAI changes: significant increase ( $z > 1.96$ ), insignificant increase ( $0 < z < 1.96$ ), insignificant decrease ( $-1.96 < z < 0$ ), significant decrease ( $z < -1.96$ ). Additionally, we calculated partial correlation coefficients between LAI and air temperature, precipitation, land surface temperature, and surface soil moisture to test the responses of LAI to hydrothermal changes. We used  $t$ -tests to test the significance level of these partial correlations and the significance level

of  $\alpha = 0.05$  ( $|t| \geq 2.101$ ) was selected to recognize the significance of partial correlations: significant positive ( $z > 2.101$ ), insignificant positive ( $0 < z < 2.101$ ), insignificant negative ( $-2.101 < z < 0$ ), significant negative ( $z < -2.101$ ). To account for the hysteresis between LAI and hydrothermal factors, we determined the lag period between shifts in LAI and hydrothermal factors using the correlation coefficient method. We calculated the correlation coefficients between LAI and hydrothermal factors for the current month and the previous 1–3 months to obtain the maximum correlation coefficients. The month with the highest correlation coefficient was used as the actual time lag for the respective LAI responses (Cai et al., 2021; Wu et al., 2015).

## 3. Results

### 3.1. Spatial patterns of LAI trend

The spatial distribution of LAI in growing season, spring, summer and autumn showed an increasing trend in 1981–2000 and 2001–2020 (Fig. 2), and the post-2000 greening trend was faster than the pre-2000 trend without considering the difference in spatial resolution. During the growing season, the areas with the large greening trend ( $>0.02 \text{ yr}^{-1}$ ) generally appeared in the northeast Yan Mountains between 1981 and 2000 (Fig. 2a). Meanwhile, the regions with a significant increase trend accounted for approximately 51 % (Fig. 2e) and only 1 % showed significant decrease trend. From 2001 to 2020 (Fig. 2f), the regions with a high greening rate ( $>0.02 \text{ yr}^{-1}$ ) were mainly distributed in the southwest Yan Mountains, and approximately 76 % of the land showed a significant increasing trend (Fig. 2j).

Regarding the three seasons, the regions with a high increasing rate ( $>0.02 \text{ yr}^{-1}$ ) of LAI in summer (Fig. 2c, h) accounted for the most (48 % for 1981–2000 and 62 % for 2001–2020), followed by spring and autumn. The significance level of LAI trend is different between 1981 and 2000 and 2001–2020. The summer LAI had the most areas with a significant increase (48 %) from 1981 to 2000 (Fig. 2e), followed by autumn (35 %) and spring (20 %). From 2001 to 2020, the regions with significant increase accounted for the most land in spring (81 %), followed by autumn (76 %) and summer (63 %) (Fig. 2j).

### 3.2. Changes in growing season LAI of different vegetation types

All seven vegetation types showed an upward trend in LAI from 1981 to 2020 (Fig. 3a). The difference in LAI among vegetation types from 1981 to 2020 was as follows: broadleaved forest ( $0.024 \text{ yr}^{-1}$ ) > cropland ( $0.014 \text{ yr}^{-1}$ ) > needle-leaved forest ( $0.01 \text{ m yr}^{-1}$ ) > grassland ( $0.009 \text{ yr}^{-1}$ ) > herbaceous cover ( $0.0086 \text{ yr}^{-1}$ ) > sparse vegetation ( $0.005 \text{ yr}^{-1}$ ) > wetlands ( $-0.004 \text{ yr}^{-1}$ ). The rate of increase in LAI before and after 2000 varied among vegetation types. Cropland had the highest increase rate ( $0.019 \text{ yr}^{-1}$ ) before 2000, while broadleaved forest had the largest increase rate ( $0.053 \text{ yr}^{-1}$ ) after 2000.

The overall increase in LAI in the Yan Mountains can be attributed to changes in the coverage of vegetation types, largely due to human land-use management (Fig. 3b). Specifically, there was a conversion of about  $12565 \text{ km}^2$  from other vegetation types (e.g., grassland, sparse vegetation, and cropland) to the forest, leading to an increasing area of broadleaved forest from 14.6 % in 1985 to 18.3 % in 2020. Meanwhile, the total area of needle-leaved forest rose from 1.28 % in 1985 to 5.25 % in 2020, an increase of about  $5208 \text{ km}^2$ . On the other hand, there was a conversion of  $3124 \text{ km}^2$  from forest to other vegetation types from 1985 to 2020 (Fig. 3b). The area of grassland decreased from 41.1 % in 1985 to 30.3 % in 2020, a decrease of about  $14139 \text{ km}^2$ . Additionally, herbaceous cover and sparse vegetation decreased by 2.6 % and 1.8 %, respectively.

### 3.3. The impact of terrain on LAI

The Yan Mountains were divided into five units at 300 m intervals to

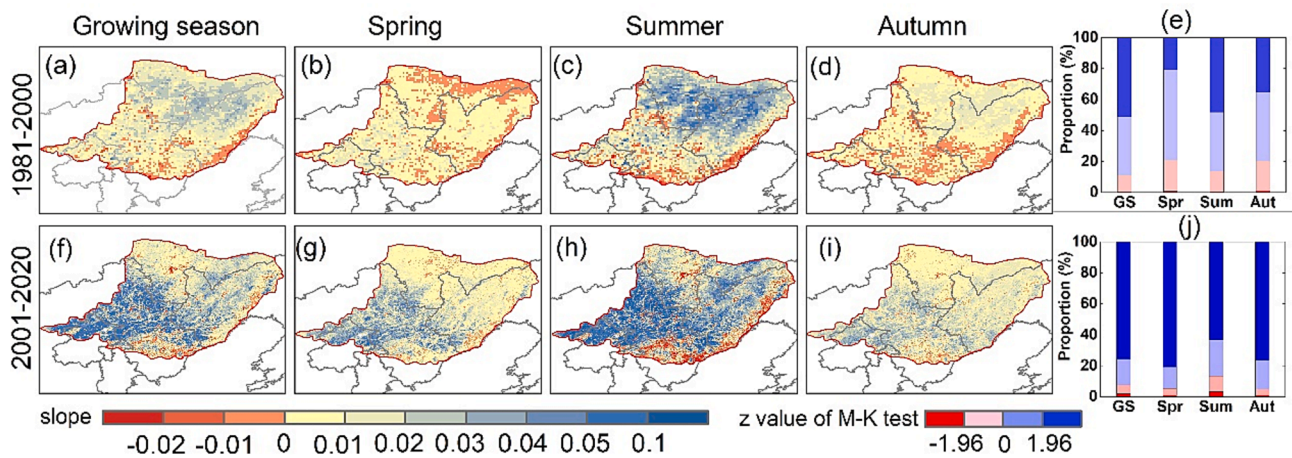


Fig. 2. Spatial distribution of the LAI trend and the proportion of the significance level (z value) in (a, e) growing season (GS), (b, f) spring (Spr), (c, g) summer (Sum), and (d, h) autumn (Aut) for 1981–2000 and 2001–2020. The significance level (z value) of LAI trends was calculated by Mann-Kendall (M–K) test, and the significance level of  $\alpha = 0.05$  ( $|z| \geq 1.96$ ) was selected to recognize the significance of LAI changes: significant increase ( $z > 1.96$ ), insignificant increase ( $0 < z < 1.96$ ), insignificant decrease ( $-1.96 < z < 0$ ), significant decrease ( $z < -1.96$ ).

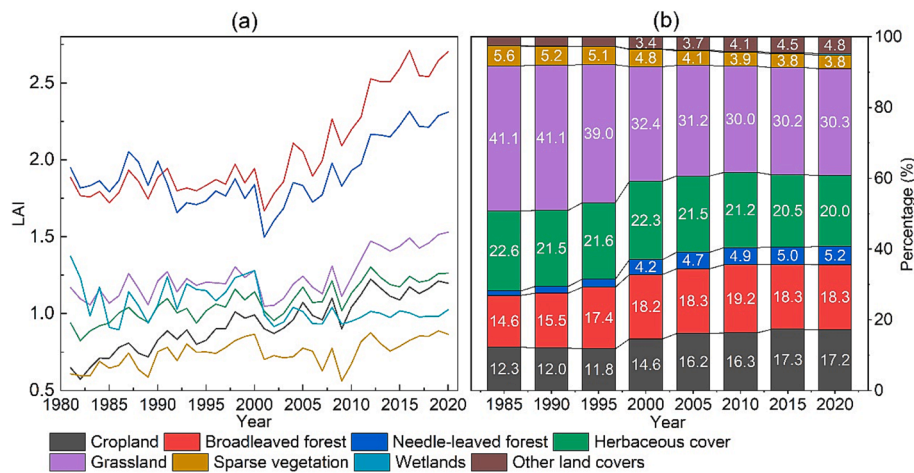


Fig. 3. (a) Inter-annual changes in LAI of different vegetation types from 1981 to 2020, and (b) shifts in the proportional coverage of different vegetation types at 5-year intervals from 1985 to 2020.

study the effect of altitude on LAI. The results showed that the LAI generally increased with increasing altitude (Fig. 4a). The highest average LAI value was found in the area above 1200 m, with an LAI value of 1.58, followed by the area between 900 and 1200 m (1.47), and the lowest was the area below 300 m (1.19). The temporal change in LAI varied at different altitudes (Fig. 4b). From 1981 to 2020, the regions

with the fastest increasing rate of LAI were located between 300 and 900 m, where cropland, grassland and broadleaved forest were the main vegetation types (Fig. S1b, c). The area with the lowest growth rate of LAI was below 300 m, primarily covered by herbaceous cover (Fig. S1a).

The increase of LAI with varied altitudes was also analyzed in Yan Mountains. In areas below 300 m, the increasing rate of LAI was 0.007

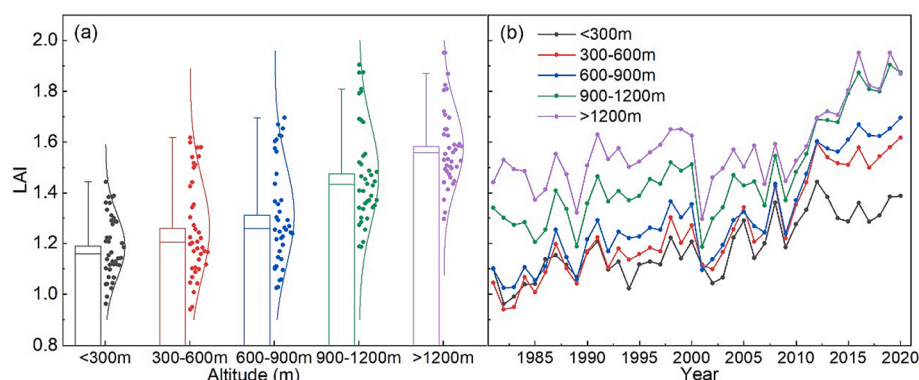


Fig. 4. Distribution of LAI at different altitude ranges (a), and interannual variation of LAI at different altitudes (b).

$\text{yr}^{-1}$  before 2000, and it was  $0.014 \text{ yr}^{-1}$  after 2000. In the area between 300 and 600 m, the LAI increasing rate was  $0.014 \text{ yr}^{-1}$  before 2000 and  $0.027 \text{ yr}^{-1}$  after 2000. The increase of cropland and broadleaved forest area largely contributed to the faster-increasing trend of LAI in this altitude range. In the area between 900 and 1200 m, the increasing rate of LAI was  $0.013 \text{ yr}^{-1}$  before 2000 and  $0.035 \text{ yr}^{-1}$  after 2000. This fast increase in LAI after 2000 was related to the increasing area of forests. Before 2000, needle-leaved forests accounted for 3.82 % of the total area, and it increased to 9.94 % after 2000 (Fig. S1d). In the areas above 1200 m, the growth rate of LAI was  $0.01 \text{ yr}^{-1}$  before 2000 and  $0.028 \text{ yr}^{-1}$  after 2000. The increase of both broadleaved forests and needle-leaved forests after 2000 largely contributed to the fast-growing LAI (Fig. S1e).

### 3.4. The influence of precipitation and air temperature on LAI

The influence of climatic conditions on LAI in the Yan Mountains showed significant differences around the year 2000. From 1981 to 2000, the inter-annual changes of LAI<sub>GS</sub> were positively correlated with precipitation across most parts of the Yan Mountains (Fig. 5a), especially in the northern parts where the partial correlation coefficients were larger than 0.6 (Fig. S2a). From 2001 to 2020, LAI showed a positive correlation with precipitation in 96 % of the region, with almost 60 % of the area having a significant positive correlation (Fig. 5e). LAI changes in spring were not significantly influenced by precipitation from 1981 to 2020 (Fig. 5b, f). The inter-annual variability of LAI in summer was most strongly affected by precipitation, with 15.40 % of the areas showing a significant positive correlation before 2000 and 33.26 % of the areas showing a significant positive correlation after 2000, mainly located in the north, east and southwest Yan Mountains. Autumn LAI and precipitation showed an insignificant correlation in most regions, with only 3.38 % and 8.44 % of the regions showing a significant positive correlation in 1981–2000 and 2001–2020, respectively. Overall, precipitation has the greatest impact on LAI in summer, followed by autumn, and LAI in spring was the least affected.

The relationships between LAI and air temperature were spatially heterogeneous. In the growing season, the regions where the correlation coefficient between LAI and air temperature greater than 0.6 (Fig. S3a) were 1.77 % of the total area from 1981 to 2000 but only 0.56 % from 2001 to 2020 (Fig. S3b). In general, LAI and air temperature in the growing season showed a positive correlation. From 1981 to 2000, 72.51 % of the regions showed a positive correlation, and 8.15 % of the regions showed a significant positive correlation (Fig. 6a). From 2001 to 2020, 69.26 % of the regions showed a positive correlation, with 3.90 % of the regions showing a significant positive correlation (Fig. 6e).

The relationship between spring LAI and air temperature was also different between 1981 and 2000 and 2001–2020. Before 2000, 1.88 % of regions showed a significant positive correlation between LAI and air temperature (Fig. 6b). After 2000, 42.53 % of regions showed a positive correlation (Fig. 6f), indicating that the change in LAI from 2000 to 2020 was more affected by temperature than from 1981 to 2000. The response of summer LAI to air temperature changed from positive to negative before and after 2000. Before 2000, 65.54 % of regions showed a positive correlation between LAI and air temperature, with 13.37 % showing a significant positive correlation, mainly in the northern part of the Yan Mountains (Fig. 6c). After 2000, 58.97 % of regions showed a negative correlation, with 3.08 % of areas showing a significant negative correlation, mainly in the northwest and east (Fig. 6g). In autumn, most areas showed no significant correlation between LAI and air temperature. During 1981–2000, 54.18 % of regions showed an insignificant positive correlation, and 45.09 % showed an insignificant negative correlation. During 2001–2020, 79.83 % of regions showed an insignificant positive correlation.

### 3.5. The influence of land surface temperature and surface soil moisture on LAI

We analyzed the response of LAI to LST and SSM from 2001 to 2020 due to the difficulty in obtaining long-term LST and SSM data. LAI was found to have a negative correlation with LST and SSM during the growing season. Approximately 63 % of the areas showed a negative correlation between LAI<sub>GS</sub> and SSM (Fig. 7a) and 92.57 % of the area showed a negative correlation between LAI<sub>GS</sub> and LST (Fig. 7b). For the spring, 52.39 % and 69.14 % of the area showed a positive correlation between LAI and SSM (Fig. 7b) and LST (Fig. 7f), respectively. During the summer, LAI and SSM (Fig. 7c) showed an insignificant correlation (13.29 % of the whole area). The correlation between summer LAI and LST was primarily negative, accounting for 71.40 % of the entire study area (Fig. 7g). In autumn, the relationship between LAI with LST and SSM was predominantly negative (Fig. 7d, h). Overall, the relationship between LAI with LST and SSM was positively correlated in spring and negative in summer and autumn.

### 3.6. Time-lag of LAI to hydrothermal conditions

An imbalance in time lag across different regions in the Yan Mountains was revealed by correlation coefficients of hydrothermal factors with LAI, as shown in Fig. 8. The lag period of LAI to hydrothermal conditions varied during different vegetation growth stages. Regarding the effects of precipitation on LAI, the vegetation growth in August had

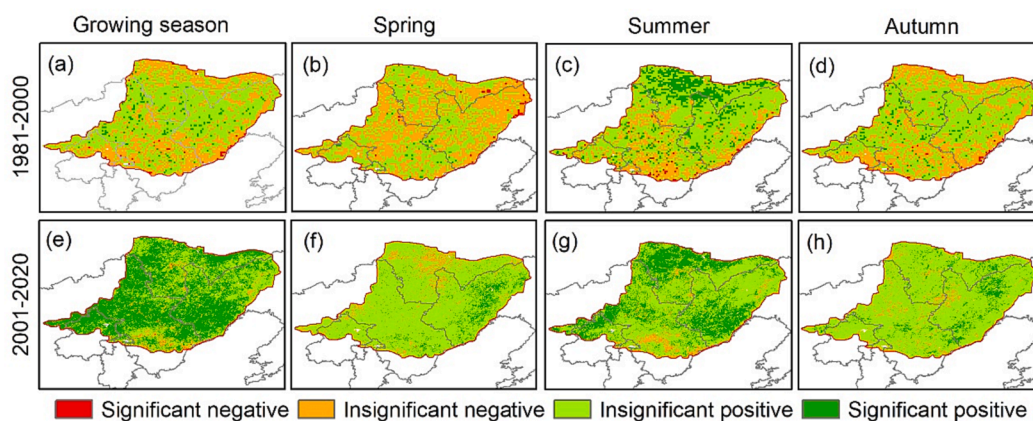


Fig. 5. Spatial patterns of the significant level (*t*-test) between LAI and precipitation in (a, e) growing season, (b, f) spring, (c, g) summer and (d, h) autumn during the periods 1981–2000 (the upper row of panels) and 2001–2020 (the lower row of panels).

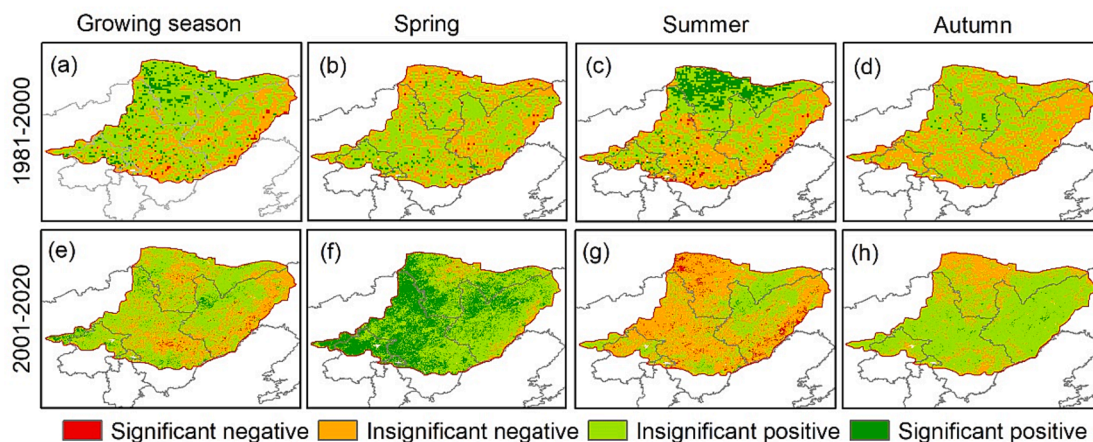


Fig. 6. Spatial patterns of the significant level ( $t$ -test) between LAI and temperature in (a, e) growing season, (b, f) spring, (c, g) summer and (d, h) autumn during the periods 1981–2000 (the upper row of panels) and 2001–2020 (the lower row of panels).

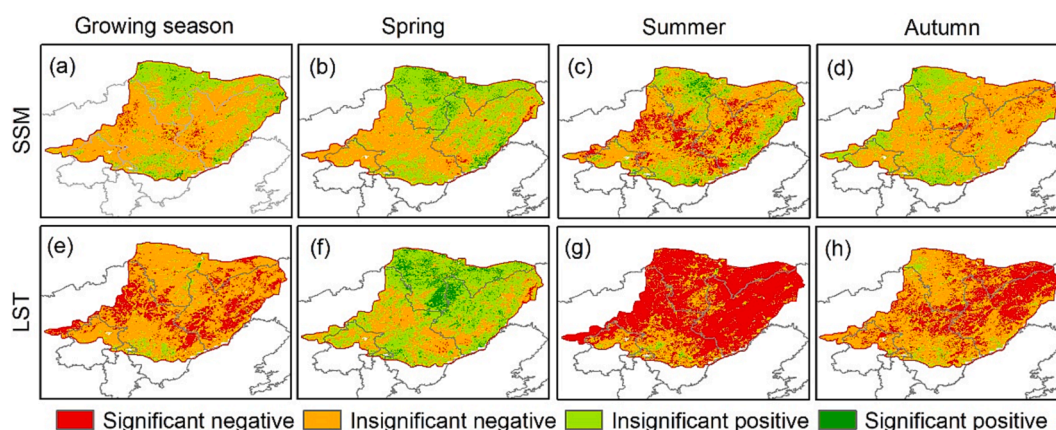


Fig. 7. Spatial patterns of the significant level between LAI and surface soil moisture (SSM) in (a) growing season, (b) spring, (c) summer and (d) autumn during the periods 2001–2020. Spatial patterns of the significant level between LAI and land surface temperature (LST) in (e) growing season, (f) spring, (g) summer and (h) autumn during the periods 2001–2020.

an immediate response to the simultaneous precipitation, with the proportion of pixels with a lag period of 0 months was 71.66 %. In other months of the growing season, there was a lag period of 1–3 months, with the longest lag in May, accounting for about 54 % of the total area, primarily located in the northwest of the Yan Mountains.

When considering the effects of air temperature on LAI, LAI had the greatest correlation with simultaneous air temperature in April and July, accounting for 51.34 % and 62.77 % of the total area, respectively. There was a lag period of over one month in other months of the growing season, with the longest lag period in June, which accounted for 55.73 % of the total area.

The LAI response to SSM showed the greatest response in May, August and September with no apparent time lag. In other months of the growing season, there was a lag period of over one month, with the largest lag period in April, accounting for 47.86 % of the total area, primarily located in the southwest Yan Mountains. Regarding the effects of LST on LAI, LAI had the greatest correlation with simultaneous LST in April, accounting for 84.59 % of the total area. There was a lag of over one month from May to October; the longest time lag (3 months) was found in July and October.

Different vegetation types exhibited varying levels of hysteresis in response to the same hydrothermal factors and to diverse climatic factors (Fig. 8). In particular, cropland, broadleaved forest, grassland, and

sparse vegetation were found to have the longest lag period in response to precipitation in May, lasting up to three months, and covering over 50 % of the total study area. However, most of the forest ecosystems, broadleaved and needle-leaved forests, did not show significant lag effects during July and August, with more than 64 % of the total grids showing no time-lag effects. Moreover, most of the vegetation types showed an immediate response to precipitation in August, with a ratio of over 63 %. Only wetlands exhibited a lagging response to precipitation, lasting more than one month and covering almost 60 % of the total area.

Most vegetation types had no lag to air temperature in April and July. However, cropland and herbaceous cover showed a lagging response to temperature in April, with a lag period of 1-month in most regions and covering 45.06 % and 48.60 % of the total area, respectively. In July, more than 56 % of the pixels showed no hysteresis effect for all vegetation types. All vegetation types were found to have a time lag to air temperature in May–June and August–October. Among them, broadleaved forest, needle-leaved forest, and grassland had the longest lag period in June, lasting three months and covering over 50 % of the total area. On the other hand, cropland, broadleaved forest, herbaceous cover, grassland, and sparse vegetation had the shortest lag period in August, lasting one month.

Regarding the effects of SSM on LAI, most vegetation types had no lag effect in May, August and September. Only broadleaved forest had a

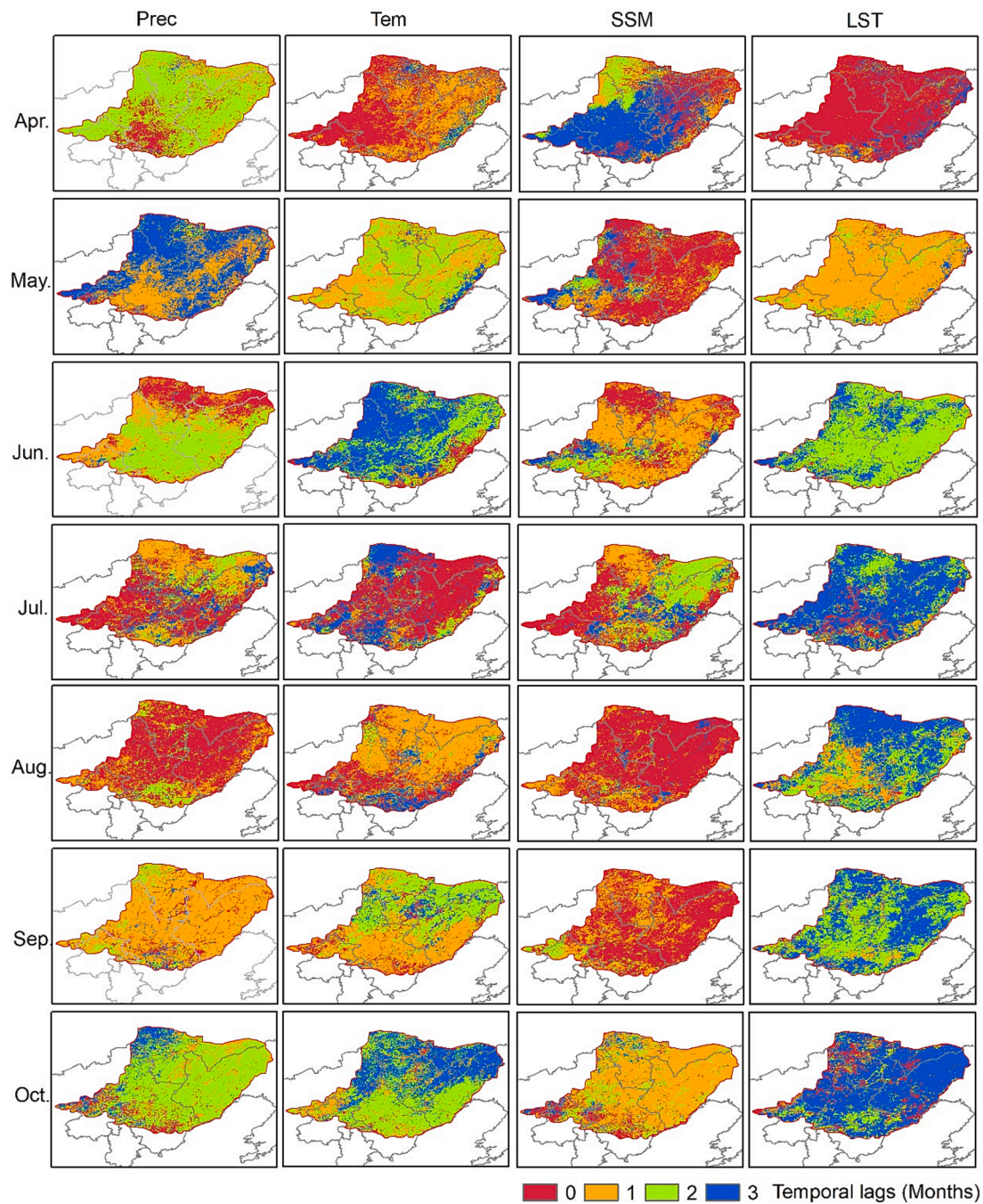


**Fig. 8.** Spatial distribution of the time lag of the LAI response to the precipitation (Prec), temperature (Tem), surface soil moisture (SSM) and land surface temperature (LST).

1-month lag to SSM in May, covering 56.13 % of the total area. Most vegetation types showed a significant lag to SSM in April, June, July and October. Among them, broadleaved forests, needle-leaved forests, and wetlands had a lag period of 3 months to SSM in April, covering over 50 % of the total area. The lag periods of cropland, broadleaved forest, herbaceous cover and grassland to SSM in June and October were mostly rather short.

Finally, we found none of the vegetation types had any hysteresis to LST in April but showed obvious hysteresis from May to October. The lag period of all vegetation types was one month in May, two months in June, and three months from July to October.

## 4. Discussion

### 4.1. Temporal trends of LAI

Analysis of GLASS LAI data showed that the Yan Mountains had a greening trend as a whole from 1981 to 2020. This finding is in line with previous studies that reported the greening trend in China using three LAI datasets (GIMMS, GLOBMAP, and GLASS) from 1982 to 2009 (Piao et al., 2015). Our results are also consistent with studies on vegetation dynamics in northern China, including parts of the Yan Mountains (Niu et al., 2019; Wang et al., 2020). However, the increasing trend of LAI in our study is larger than the results reported by Niu et al. (2019), probably because of differences in spatial extent. Although LAI showed an

increasing trend throughout the growing season, the fluctuations of LAI in different seasons were significantly different (Fig. S4). Vegetation in summer was always at the peak of LAI from 1981 to 2020. Autumn LAI was larger than spring LAI except for 2009 and 2014, which may be caused by the extremely low precipitation in summer (Fig. S5).

Our study also found that the area of forests has increased significantly from 1981 to 2020, with about 12562 km<sup>2</sup> of land changing from other vegetation types, such as grassland, sparse vegetation, herbaceous cover, and cropland, to forests. This greening trend has been attributed to afforestation (Chen et al., 2020; Lin et al., 2020; Piao et al., 2019) and may be linked to China's national ecological protection policy (Winkler et al., 2021). Since 2000, the Chinese government has implemented several ecological restoration projects, such as the Three-Norths Shelter Forest Project and Beijing-Tianjin Sandstorm-control Program, to restore the degraded environment caused by deforestation and soil loss (Ouyang et al., 2016; Pei et al., 2021; Wang et al., 2020).

The spatial heterogeneity of LAI change trends in the Yan Mountains is evident. The areas displaying a greening trend were primarily located in the northeast before 2000 and in the southwest after 2000. Before 2000, the air temperature and precipitation showed no significant increase in the northeast, indicating that hydrothermal conditions were not the cause of the observed increase in LAI in these areas. This increase may instead be attributed to human management practices, such as fertilization and irrigation of farmland (Zhu et al., 2016). After 2000, there was no significant increase in air temperature and precipitation in the southwest Yan Mountains. Therefore, these factors cannot explain the observed increase in LAI in these regions. This increase may be related to national policies and human factors, such as reforestation.

#### 4.2. The effects of topography and land cover change on LAI

Variations in topography and land use cover can affect the temporal change in LAI. Topographic variation results in micro-environment and biological gradients, which in turn affect the spatial distribution and patterns of vegetation (Li et al., 2021). In the Yan mountains, vegetation LAI generally increased with increasing altitude, which aligns with the findings of Zhang et al., (2021a). The change rate in LAI at different altitudes was also different, with the area located between 300 and 900 m experiencing a more significant increase than the areas below 300 m and above 900 m. This may be caused by the increasing area of forests and crop and the decreasing of grassland in these regions (Fig. S1 b, c). Land cover change is also a crucial factor that influences the temporal changes in LAI (Niu et al., 2019; Piao et al., 2019). According to Winkler et al. (2021), global land cover changes are four times greater than previously estimated. The Yan Mountains have also experienced significant land cover changes, especially after the Chinese government implemented various ecological protection policies (Chen et al., 2019a; Chen et al., 2020). The forest area has increased significantly, with about 12562 km<sup>2</sup> of land changing from other vegetation types to forest. As a result, the forest LAI showed the most significant increase among all vegetation types in Yan Mountains over the past four decades.

#### 4.3. The relationship between the greening trend and hydrothermal conditions

Vegetation variety is affected by both climatic and anthropogenic factors (Guo et al., 2021; Yin et al., 2022). Climatic factors, particularly temperature and precipitation, play a direct or indirect role in determining the greenness of vegetation. Furthermore, land surface temperature and soil moisture are impacted not only by changes in precipitation but also by temperature and radiation (Li et al., 2015). Therefore, climatic and land surface hydrothermal conditions are closely tied to terrestrial vegetation ecosystems.

Regarding the relationships with hydrothermal conditions, vegetation in the Yan Mountains was more relative to precipitation than to air temperature (Figs. 5, 6), which is consistent with findings from other

studies in northern China (Sun et al., 2021; Sun et al., 2015). During the period 1981–2020, there were more regions with a positive correlation between LAI<sub>GS</sub> and precipitation compared to regions with a positive correlation between LAI<sub>GS</sub> and temperature, which suggests that the vegetation growth was largely driven by precipitation (Chu et al., 2019; Xu et al., 2017). On a seasonal scale, LAI and air temperature in spring showed a noticeable positive correlation after 2000 (Fig. S3f). This indicates that an increase in spring temperature could promote the greening of vegetation (Guo et al., 2021). During the summer months, LAI and air temperature showed a negative correlation from 2001 to 2020 (Fig. S3g), probably because high temperatures caused vegetation transpiration and land surface evapotranspiration (Chu et al., 2019). However, from 1981 to 2000, summer LAI and air temperature showed a positive correlation in Tongliao City (Fig. S3c), which may be due to the significant increase in precipitation in this area. Abundant precipitation and moderate increases in temperature can facilitate plant photosynthesis and leaf growth.

Further, regarding the land surface hydrothermal conditions, the correlation between vegetation LAI with soil moisture and surface temperature was negative during the growing season in most regions. This negative was probably due to soil moisture of decreased precipitation and increased evaporative water demand caused by rising air temperature and land surface temperature (Li et al., 2022). From 2001 to 2020, the trend of vegetation greenness (LAI) was upward, while surface soil moisture (SSM) showed a downward trend, potentially as a result of afforestation and climate changes. Several studies have indicated that afforestation can lead to a decrease in soil moisture (Jia and Shao, 2014; Jian et al., 2015). On a seasonal scale, the correlation between LAI and surface temperature was stronger in spring than with soil moisture, and an increase in surface temperature was beneficial for vegetation growth. In contrast, during summer and autumn, vegetation greenness was negatively correlated with land surface temperature. An increase in land surface temperature would increase plant transpiration and surface evaporation, reducing available water for vegetation.

#### 4.4. The time-lag effects between LAI and climatic factors

The relationship between vegetation growth and climate is complex, with a delay in responses when climate changes are beyond the tolerance of vegetation (Zhao et al., 2020). This phenomenon is known as hysteresis. We found that the hysteresis period between vegetation growth and hydrothermal conditions varies across different growth stages of vegetation. During the early (April to June) and late (October) stages of the growing season, there was a time lag of 2–3 months in vegetation response to changes in air temperature and precipitation, which differed in findings at the Loess Plateau (Zhao et al., 2020). This discrepancy may be due to the different climatic conditions in the study area, as the Yan Mountains are in a semi-humid region, while the Loess Plateau is a semi-arid region. In the mid-growing season (July and September), there was a 0–1 month lag in the response of vegetation to changes in air temperature and precipitation. Notably, there was no delayed response of vegetation to precipitation in August and to air temperature in July.

As a result of ongoing climate change, the surface soil moisture and land surface temperature are also constantly changing, which directly influences vegetation growth (Li et al., 2022; Wang et al., 2018). We found that the hysteresis period of vegetation in response to SSM and LST differs from that in response to air temperature and precipitation. During the growing season, the time lag of LAI in response to SSM was shorter than that in response to precipitation, and the time lag of LAI in response to LST was longer than that in response to air temperature. In April, vegetation showed a time lag of three months in response to SSM, while there was no time lag between LAI and LST. Hence, the increased temperature was found to be more significant than moisture in the early stage of vegetation growth.

## 5. Conclusion

In this study, we analyzed the spatial and temporal variability of LAI in the Yan Mountains between 1981 and 2020 using the GLASS LAI dataset and evaluated the effects of meteorological and land surface hydrothermal conditions on LAI. Our results showed an overall greening trend of vegetation in the Yan Mountains, characterized by an increase in LAI. The trend of vegetation was more pronounced after the year 2000 and varied between different vegetation types and altitudes. Our study illustrates that it is crucial to consider both the impact of hydrothermal changes and human activities when studying changes in LAI. Our results indicate that surface thermal and moisture conditions have a negative impact on LAI, while climatic conditions have a mostly positive effect. Additionally, the time lag of vegetation response to changes in surface hydrothermal conditions is typically shorter than vegetation response to air temperature and precipitation. Our study provides valuable insights into how vegetation dynamics in the Yan Mountains have changed in response to hydrothermal conditions over the past several decades. This information can support the Chinese government in developing more effective and ecology-based vegetation protection policies.

## CRedit authorship contribution statement

**Da Guo:** Conceptualization, Methodology, Formal analysis, Writing – original draft. **Xiaoning Song:** Supervision, Funding acquisition. **Ronghai Hu:** Resources, Writing – review & editing, Funding acquisition. **Rui Ma:** Data curation, Visualization. **Yanan Zhang:** Data curation, Writing – review & editing. **Liang Gao:** Investigation, Resources. **Xinming Zhu:** Methodology, Software. **Paul Kardol:** Writing – review & editing.

## Declaration of Competing Interest

The authors declare that they have no known competing financial interests or personal relationships that could have appeared to influence the work reported in this paper.

## Data availability

Data will be made available on request.

## Acknowledgements

This work was supported by the Third Xinjiang Scientific Expedition Program (Grant No. 2022xjkk0402), Beijing Nova Program of Science and Technology, China (Grant No. Z191100001119132) and the Fundamental Research Funds for the Central Universities. We thank National Earth System Science Data Center, Google Earth Engine, Copernicus Climate Change Service, Resource and Environment Science and Data Center and CASEarth for providing the essential data for our study. We also sincerely thank all the anonymous reviewers for their insightful comments and suggestions in the manuscript.

## Appendix A. Supplementary data

Supplementary data to this article can be found online at <https://doi.org/10.1016/j.ecolind.2023.111291>.

## References

Duo, A., Zhao, W., Qu, X., Jing, R., Xiong, K., 2016. Spatio-temporal variation of vegetation coverage and its response to climate change in North China plain in the last 33 years. *Int. J. Appl. Earth Obs. Geoinf.* 53, 103–117.

Afuye, G.A., Kalumba, A.M., Busayo, E.T., Orimoloye, I.R., 2022. A bibliometric review of vegetation response to climate change. *Environ. Sci. Pollut. Res.* 29, 18578–18590.

Antala, M., Juszczak, R., van der Tol, C., Rastogi, A., 2022. Impact of climate change-induced alterations in peatland vegetation phenology and composition on carbon balance. *Sci. Total Environ.* 827, 154294.

Baret, F., Hagolle, O., Geiger, B., Bicheron, P., Miras, B., Huc, M., et al., 2007. LAI, fAPAR and fCover CYCLOPES global products derived from VEGETATION. *Remote Sens. Environ.* 110, 275–286.

Cai, S., Song, X., Hu, R., Guo, D., 2021. Ecosystem-dependent responses of vegetation coverage on the tibetan plateau to climate factors and their lag periods. *ISPRS Int. J. Geo Inf.* 10.

Chen, J.M., Black, T.A., 1992. Defining leaf area index for non-flat leaves. *Plant Cell Environ.* 15, 421–429.

Chen, Y., Chen, L., Cheng, Y., Ju, W., Chen, H.Y.H., Ruan, H., 2020. Afforestation promotes the enhancement of forest LAI and NPP in China. *For. Ecol. Manage.* 462.

Chen, J.M., Ju, W., Ciaisi, P., Viovy, N., Liu, R., Liu, Y., et al., 2019b. Vegetation structural change since 1981 significantly enhanced the terrestrial carbon sink. *Nat. Commun.* 10, 4259.

Chen, C., Park, T., Wang, X., Piao, S., Xu, B., Chaturvedi, R.K., et al., 2019a. China and India lead in greening of the world through land-use management. *Nat. Sustainability* 2, 122–129.

Chu, H., Venevsky, S., Wu, C., Wang, M., 2019. NDVI-based vegetation dynamics and its response to climate changes at Amur-Heilongjiang River Basin from 1982 to 2015. *Sci. Total Environ.* 650, 2051–2062.

Gang, C., Zhou, W., Chen, Y., Wang, Z., Sun, Z., Li, J., et al., 2014. Quantitative assessment of the contributions of climate change and human activities on global grassland degradation. *Environ. Earth Sci.* 72, 4273–4282.

Guo, D., Song, X., Hu, R., Cai, S., Zhu, X., Hao, Y., 2021. Grassland type-dependent spatiotemporal characteristics of productivity in Inner Mongolia and its response to climate factors. *Sci. Total Environ.* 775.

Jia, Y., Shao, M., 2014. Dynamics of deep soil moisture in response to vegetational restoration on the Loess Plateau of China. *J. Hydrol.* 519, 523–531.

Jian, S., Zhao, C., Fang, S., Yu, K., 2015. Effects of different vegetation restoration on soil water storage and water balance in the Chinese Loess Plateau. *Agric. for. Meteorol.* 206, 85–96.

Jiang, H., Xu, X., Guan, M., Wang, L., Huang, Y., Jiang, Y., 2020. Determining the contributions of climate change and human activities to vegetation dynamics in agro-pastoral transitional zone of northern China from 2000 to 2015. *Sci. Total Environ.* 718, 134871.

Jin, H., Li, A., Bian, J., Nan, X., Zhao, W., Zhang, Z., et al., 2017. Intercomparison and validation of MODIS and GLASS leaf area index (LAI) products over mountain areas: a case study in southwestern China. *Int. J. Appl. Earth Obs. Geoinf.* 55, 52–67.

Li, W., 2004. Degradation and restoration of forest ecosystems in China. *For. Ecol. Manage.* 201, 33–41.

Li, Z., Chen, Y., Li, W., Deng, H., Fang, G., 2015. Potential impacts of climate change on vegetation dynamics in Central Asia. *J. Geophys. Res. Atmos.* 120, 12345–12356.

Li, P., Hu, Z., Liu, Y., 2020. Shift in the trend of browning in Southwestern Tibetan Plateau in the past two decades. *Agric. for. Meteorol.* 287.

Li, W., Migliavacca, M., Forkel, M., Denissen, J.M.C., Reichstein, M., Yang, H., et al., 2022. Widespread increasing vegetation sensitivity to soil moisture. *Nat. Commun.* 13, 3959.

Li, C., Qi, J., Yang, L., Wang, S., Yang, W., Zhu, G., et al., 2014. Regional vegetation dynamics and its response to climate change—a case study in the Tao River Basin in Northwestern China. *Environ. Res. Lett.* 9.

Li, P., Wang, J., Liu, M., Xue, Z., Bagherzadeh, A., Liu, M., 2021. Spatio-temporal variation characteristics of NDVI and its response to climate on the Loess Plateau from 1985 to 2015. *Catena* 203.

Lin, X., Niu, J., Berndtsson, R., Yu, X., Zhang, L., Chen, X., 2020. NDVI dynamics and its response to climate change and reforestation in Northern China. *Remote Sens. (basel)* 12.

Ma, M., Frank, V., 2007. Interannual variability of vegetation cover in the Chinese Heihe River Basin and its relation to meteorological parameters. *Int. J. Remote Sens.* 27, 3473–3486.

Mao, D., Wang, Z., Luo, L., Ren, C., 2012. Integrating AVHRR and MODIS data to monitor NDVI changes and their relationships with climatic parameters in Northeast China. *Int. J. Appl. Earth Obs. Geoinf.* 18, 528–536.

Myneni, R., Knyazikhin, Y., Park, T., 2015. MOD15A2H MODIS leaf area Index/FPAR 8-Day L4 global 500m SIN grid V006. NASA EOSDIS Land Processes DAAC.

Niu, Q., Xiao, X., Zhang, Y., Qin, Y., Dang, X., Wang, J., et al., 2019. Ecological engineering projects increased vegetation cover, production, and biomass in semiarid and subhumid Northern China. *Land Degrad. Dev.* 30, 1620–1631.

Ouyang, Z., Zheng, H., Xiao, Y., Polasky, S., Liu, J., Xu, W., et al., 2016. Improvements in ecosystem services from investments in natural capital. *Science* 352, 1455–1459.

Pei, H., Liu, M., Jia, Y., Zhang, H., Li, Y., Xiao, Y., 2021. The trend of vegetation greening and its drivers in the Agro-pastoral ecotone of northern China, 2000–2020. *Ecol. Ind.* 129.

Peng, S., Ding, Y., Liu, W., Li, Z., 2019. 1 km monthly temperature and precipitation dataset for China from 1901 to 2017. *Earth Syst. Sci. Data* 11, 1931–1946.

Peng, J., Loew, A., Merlin, O., Verhoest, N.E.C., 2017. A review of spatial downscaling of satellite remotely sensed soil moisture. *Rev. Geophys.* 55, 341–366.

Piao, S., Fang, J., Zhou, L., Guo, Q., Henderson, M., Ji, W., 2003. Interannual variations of monthly and seasonal normalized difference vegetation index (NDVI) in China from 1982 to 1999. *J. Geophys. Res.* 108.

Piao, S., Mohammat, A., Fang, J., Cai, Q., Feng, J., 2006. NDVI-based increase in growth of temperate grasslands and its responses to climate changes in China. *Glob. Environ. Chang.* 16, 340–348.

- Piao, S., Yin, G., Tan, J., Cheng, L., Huang, M., Li, Y., et al., 2015. Detection and attribution of vegetation greening trend in China over the last 30 years. *Glob. Chang. Biol.* 21, 1601–1609.
- Piao, S., Wang, X., Park, T., Chen, C., Lian, X., He, Y., et al., 2019. Characteristics, drivers and feedbacks of global greening. *Nature Reviews Earth & Environment* 1, 14–27.
- Sun, R., Chen, S., Su, H., 2021. Climate dynamics of the spatiotemporal changes of vegetation NDVI in Northern China from 1982 to 2015. *Remote Sens. (basel)* 13.
- Sun, Y., Yang, Y., Zhang, Y., Wang, Z., 2015. Assessing vegetation dynamics and their relationships with climatic variability in northern China. *Physics and Chemistry of the Earth, Parts a/b/c* 87–88, 79–86.
- Tucker, C., Fung, I.Y., Keeling, C., Gammon, R., 1986. Relationship between atmospheric CO<sub>2</sub> variations and a satellite-derived vegetation index. *Nature* 319, 195–199.
- Wang, G., Innes, J.L., Lei, J., Dai, S., Wu, S.W., 2007. China's forestry reforms. *Science* 318, 1556–1557.
- Wang, H., Sun, B., Yu, X., Xin, Z., Jia, G., 2020. The driver-pattern-effect connection of vegetation dynamics in the transition area between semi-arid and semi-humid northern China. *Catena* 194.
- Wang, X., Wang, B., Xu, X., Liu, T., Duan, Y., Zhao, Y., 2018. Spatial and temporal variations in surface soil moisture and vegetation cover in the Loess Plateau from 2000 to 2015. *Ecol. Ind.* 95, 320–330.
- Wang, Y., Zhang, Z., Chen, X., 2021. Quantifying influences of natural and anthropogenic factors on vegetation changes based on geodetector: a case study in the Poyang Lake Basin China. *Remote Sensing* 13.
- Winkler, K., Fuchs, R., Rounsevell, M., Herold, M., 2021. Global land use changes are four times greater than previously estimated. *Nat. Commun.* 12, 2501.
- Wu, D., Zhao, X., Liang, S., Zhou, T., Huang, K., Tang, B., et al., 2015. Time-lag effects of global vegetation responses to climate change. *Glob. Chang. Biol.* 21, 3520–3531.
- Xiao, Z., Liang, S., Wang, J., Chen, P., Yin, X., Zhang, L., et al., 2014. Use of general regression neural networks for generating the GLASS leaf area index product from time-series MODIS surface reflectance. *IEEE Trans. Geosci. Remote Sens.* 52, 209–223.
- Xu, H.J., Wang, X.P., Yang, T.B., 2017. Trend shifts in satellite-derived vegetation growth in Central Eurasia, 1982–2013. *Sci. Total Environ.* 579, 1658–1674.
- Yan, G., Hu, R., Luo, J., Weiss, M., Jiang, H., Mu, X., et al., 2019. Review of indirect optical measurements of leaf area index: Recent advances, challenges, and perspectives. *Agric. for. Meteorol.* 265, 390–411.
- Yin, Y., Deng, H., Ma, D., 2022. Complex effects of moisture conditions and temperature enhanced vegetation growth in the Arid/humid transition zone in Northern China. *Sci. Total Environ.* 805, 150152.
- Zhang, W., Jin, H., Shao, H., Li, A., Li, S., Fan, W., 2021. Temporal and spatial variations in the leaf area index and its response to topography in the three-river source region China from 2000 to 2017. *ISPRS Int. J. Geo Inf.* 10.
- Zhang, X., Liu, L., Chen, X., Gao, Y., Xie, S., Mi, J., 2021. GLC\_FCS30: global land-cover product with fine classification system at 30 m using time-series Landsat imagery. *Earth Syst. Sci. Data* 13, 2753–2776.
- Zhao, J., Huang, S., Huang, Q., Wang, H., Leng, G., Fang, W., 2020. Time-lagged response of vegetation dynamics to climatic and teleconnection factors. *Catena* 189.
- Zhu, Z., Bi, J., Pan, Y., Ganguly, S., Anav, A., Xu, L., et al., 2013. Global data sets of vegetation leaf area index (LAI)3g and fraction of photosynthetically active radiation (FPAR)3g derived from global inventory modeling and mapping studies (GIMMS) normalized difference vegetation index (NDVI3g) for the period 1981 to 2011. *Remote Sens. (basel)* 5, 927–948.
- Zhu, Z., Piao, S., Myneni, R.B., Huang, M., Zeng, Z., Canadell, J.G., et al., 2016. Greening of the Earth and its drivers. *Nat. Clim. Chang.* 6, 791–795.
- Zhu, Z., Piao, S., Lian, X., Myneni, R.B., Peng, S., Yang, H., 2017. Attribution of seasonal leaf area index trends in the northern latitudes with “optimally” integrated ecosystem models. *Glob. Chang. Biol.* 23, 4798–4813.